The Design of a Novel Approach for the Assessment of Thermal Insulation in Buildings Using Infrared Thermography and Artificial Intelligence

Arijit Sen and Amin Al-Habaibeh*

Product Design

Innovative and Sustainable Built Environment Technologies Research Group (iSBET)

Nottingham Trent University, UK

Arijit.Sen2016@my.ntu.ac.uk and Amin.Al-Habaibeh@ntu.ac.uk

*Corresponding author, Professor Amin Al-Habaibeh, Amin.Al-Habaibeh@ntu.ac.uk

Biography

Arijit Sen

Arijit is a PhD Researcher at Nottingham Trent University, pursuing his research work in the field of energy in buildings and sustainability innovation. He received his BSc in Industrial and Production Engineering from Shah Jalal University of Science and Technology and his MSc in Advanced Product Design Engineering with distinction from Nottingham Trent University. He worked for more than 6 years as a member of staff in the Department of Mechanical Engineering at IUBAT – International University of Business Agriculture and Technology and also worked as a guest lecturer at Upper Austria University of Applied Sciences.

Amin Al-Habaibeh

Amin has been appointed as Professor of Intelligent Engineering Systems within the Product Design team at Nottingham Trent University since August 2014. He is also the Director of DTA-Energy (Doctoral Training Alliance). His research and teaching activities focus on several multi-disciplinary topics in the broad area of product design, automation, energy and artificial intelligence. Amin is currently leading the Innovative and Sustainable Built Environment Technologies research group (iSBET) and co-founder of the Advance Design and Manufacturing Engineering Centre (ADMEC). Amin holds a BSc degree from the University of Jordan in Industrial Engineering (Manufacturing and Design),

an MSc degree from University of Nottingham in Manufacturing Systems and a PhD degree in Advanced Manufacturing Technologies from the University of Nottingham.

Abstract

Buildings consume high energy for space and water heating, and thereby contribute largely to greenhouse gas emission. Improving thermal insulation of building's walls can significantly reduce energy consumption for space heating as well as decrease greenhouse gas emission. However, prior to the retrofitting of a building it is required to evaluate the current level of wall insulation, as over insulation will increase the cost of insulation and decrease the expected energy savings; and hence causing a lengthy payback period. Infrared thermography is a very effective tool in evaluating building's thermal performance when a reasonable temperature gradient exists between indoor and outdoor environment. This paper presents a novel design which involves using low-resolution infrared camera with single point heating system from which the thermal conductivity and thermal insulation of building's wall can be categorised and estimated. An experimental study has been conducted on different sample wall sections and Artificial Neural Network is used to analyse the infrared images of walls for categorisation based on the level of wall insulation. The result shows 88% overall accuracy in categorizing the wall types based on their level of insulation from a set of infrared images.

Keywords: Insulation**;** U-value; Artificial intelligence; Neural Network; Infrared Thermography.

1. Introduction

Worldwide energy demand is increasing with the economic and population growth (OECD, 2011); however, the energy production is still largely dependent on fossil fuel (BP, 2018). Burning of fossil fuel releases a massive amount of greenhouse gases, which results in an increased risk of climate change. The UK government initially set the target of limiting greenhouse gas emission at 20% of the 1990's level by 2050 to support the pledge of The Paris Agreement (Committee on Climate Change, 2016) and now the target is revised net zero greenhouse gas emission by 2050 (Department for Business Energy & Industrial Strategy, 2019). Domestic sector is the second highest energy-consuming sector in the UK after transport sector; and space and water heating is responsible for 80% of the energy consumption in this sector (BEIS, 2018). Therefore, it is necessary to develop strategies for reducing the energy consumption due to space heating in residential buildings. Retrofitting of an existing building with improved wall insulation can reduce heat loss through the building's walls and consequently energy consumption for space heating. However, before the

retrofitting, it is necessary to identify the current level of insulation, presented by the U-value of the building's wall.

The designed U-value of a building's wall is calculated as the reciprocal of the summation of thermal resistances of different layers of the wall (Gaspar, Casals and Gangolells, 2016).

$$U = \frac{1}{R_i + \frac{d_1}{k_1} + \frac{d_2}{k_2} + \cdots\cdots\cdots + R_e} \qquad (1)$$

Here, U is the U-value of the wall; k is the thermal conductivity of the materials in different layers of the wall; d is the thickness of the wall layers; R_i and R_e are the thermal resistance of air at internal surface and external surface respectively. From the theoretical values of the thermal conductivities of wall layers and their thickness, the designed U-value of a building's wall can be estimated. However, over long periods of time, the material properties of wall layers degrade and it could lead to a difference between the designed and in-situ U-values as high as 153% due to the inaccurate knowledge of the wall stratigraphy (Evangelisti *et al.*, 2015). Therefore, in-situ U-value estimation is required, particularly, for the old buildings, as the other method tends to overestimate the U-value (Lucchi, 2017). It can be done by conducting laboratory test on the samples collected by drilling the walls. However, it results in making holes in the wall. There are several devices available to measure U-values of test specimen in laboratory; however, these often differ as high as 30% from the in-situ U-value (Doran, 2001). There are two non-invasive methods currently exist for in-situ U-value measurement namely Heat Flux Meter (HFM) method and Infrared Thermovision Technique (ITT). The net heat flux through a building's wall is proportional to its U-value and the temperature gradient between indoor and outdoor environment; hence, the U-value can be determined by measuring the heat flux, indoor temperature and outdoor temperature using a heat flux meter and temperature sensors respectively (Gaspar, Casals and Gangolells, 2016). A heat flux meter contains a sensor body with known thickness and thermal conductivity, and by measuring the temperature difference between two sides of that sensor body the heat flux is determine (Campbell Scientific, 2012). To obtain a reasonable accuracy in this method more than 10^{o}C difference between indoor and outdoor temperature is required, as at low temperature difference the heat flux through the wall falls below the sensible range of heat flux meter (Ficco *et al.*, 2015). Moreover, it requires at least 72 consecutive hours of data acquisition (Nardi, Sfarra and Ambrosini, 2014). And it is sometimes difficult to place the

sensors at a suitable place in an occupied house, which results in inaccurate estimation of U-value (Li *et al.*, 2015). For example, Baker (2008) used HFM methods to measure U-value of traditional Scottish buildings; however, their work was limited to painted walls only as it may damage the wallpaper. Heat flux meter attached to a wall actually measures the heat flux through itself from room environment than through the wall; and hence it would be better to place the heat flux meter inside the wall or plastered on the wall surface (Desogus, Mura and Ricciu, 2011). However, this process may damage the wall. In addition, statistical inference using Bayesian analyses was introduce by some researcher (Biddulph *et al.*, 2014 and Gori *et al.*, 2017) to enhance the performance of heat flux; however, it still requires to satisfy the condition of maintaining 10^{o}C thermal gradient and having 72 hours of data acquisition. ITT method estimates the U-value as a ratio of total thermal power and the temperature difference between indoor and outdoor environment, where the thermal power is determined by summing up the heat dissipated from external surface of a building's wall by means of convection and radiation (Albatici and Tonelli, 2010). The indoor and outdoor temperature are measured from an infrared image, which is captured with a partially open window in the wall for a very short period during the time of image capture. ITT is faster method than HFM; however, it requires the measurement to be performed at night, preferably in overcast condition to avoid effect of solar radiation, and it also requires more than 10^{o}C temperature difference between indoor and outdoor environment (Albatici, Tonelli and Chiogna, 2015). Significant efforts have been made to compare U-value measured using ITT method with that of HFM method. For example, Fokaides and Kalogirou (2011) found U-value estimated using ITT method is very close to that of HFM method. Nardi, Sfarra and Ambrosini (2014) found ITT methods has as low as 2% difference with U-value measured in HFM method if the experiment is done on overcast condition. However, for sunny days the difference goes as high as 37%. In case of the experimentation using guarded hot box in laboratory, the ITT method shows 3% to 7% deviation from designed U-value whereas, for HFM method it is around 10% (Nardi *et al.*, 2015). As the material properties of the test specimen used in laboratory experiments is not subject to degradation, the designed U-value is the benchmark in this case. Therefore, it can be stated that ITT method has better accuracy over HFM method. The reliable estimation of in-situ U-value is difficult in real buildings because of many constraints such as, installing instruments, extended period of monitoring time, dependency on season, dependency on weather condition and presence of sunlight. Infrared thermography is a robust technology used in many cases to evaluate the thermal performance of buildings. It has been used for thermal bridge detection (Kylili *et al.*, 2014), (Asdrubali,

Baldinelli and Bianchi, 2012), heat loss estimation through doors (Al-Habaibeh, Medjdoub and Pidduck, 2012), detection of energy related defects in buildings (Fox *et al.*, 2014), evaluating energy performance of buildings (Al-Habaibeh and Siena, 2012) and so on. Furthermore, thermography has the versatility in measuring large building area as well as capability to point out imprecation in building's wall (Danielski and Fröling, 2015). Artificial intelligence has been successfully used for thermal characterisation of wall (Sassine, 2016) and detection of thermal diffusivity of insulating materials (Chudzik, 2012). Therefore, combining artificial intelligence with infrared thermography could overcome the limitations of estimating in-situ U-value for building's wall. This paper proposes a novel approach of categorisation of buildings' wall based on the U-value by combining thermal images of walls and artificial intelligence with the application of point heat.

2. Methodology

An uninsulated wall has a relatively high U-value and most of the applied heat will pass through it. Conversely, an insulated wall has a low U-value and most of the applied heat will disperse over the internal surface. The difference in the thermal response, while applying a point heat in the internal side of a test wall for a certain period, can be observed by monitoring the wall using a low-resolution infrared camera.

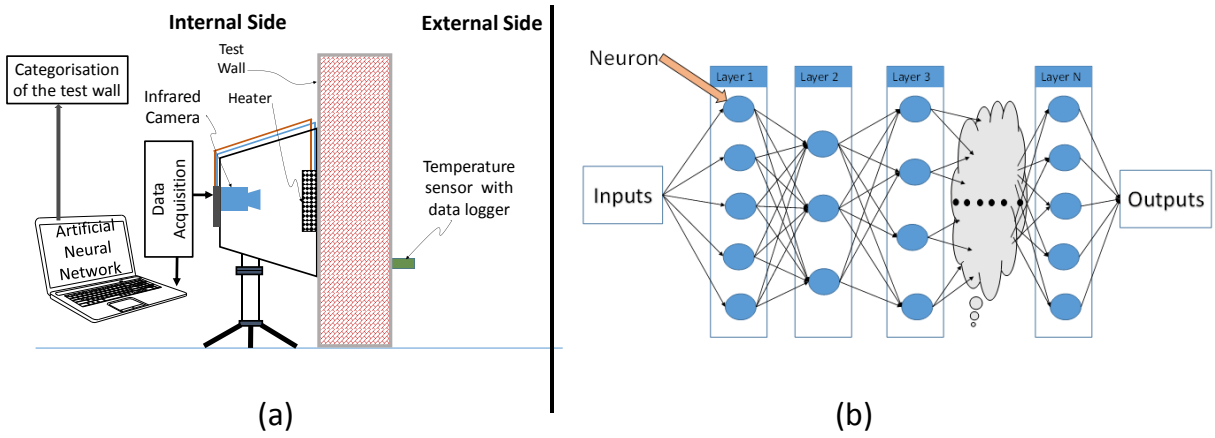

Figure 1: (a) schematic diagram of experimental set up, (b) the architecture of a typical ANN

The schematic diagram of the experimental set up is shown in Figure 1(a). The thermal profile generated from the infrared images is used to train an Artificial Neural Network (ANN) for the categorisation of wall type. A typical ANN architecture is shown in Figure 1(b). ANN consists of neurons organised in layers which mimic the thought process of human brain. The

core of a neuron in ANN contains a transfer function preceded by weights and bias. ANN can be trained to learn the features in a data set and based on the learning it can predict the output of a similar unknown input. The training is an iterative process and during the training the weights and biases in the neurons are updated based on a cost function. The objective of the cost function is to minimise the error gradient. In this way, the ANN maps the relationship between input and output data set and learn the feature in the data. The automated learning process of neurons is the main advantage of ANN over statistical methods to explain the complex and nonlinear relationship. However, it leads to the risk of overfitting as well (Tu, 1996). This is because an ANN arbitrarily selects the initial weights and biases in neurons and that leads to producing different output every time. The simple way to overcome this problem is to train the network several times and the mean value of the ANN performance give a generalised solution (Beale, Hagan and Demuth, 2017). The experiment is conducted twice on each wall type so that the data obtained from the first run of the experiment could be used for training the ANN and the data obtained from the second run of experiment can be used to test the network performance. The ANN is trained 25 times and the average performance is considered at the network's performance.

3. Experimental work

The experimental work was conducted on four different wall samples made of brick, brick with external insulation, concrete block and concrete block with external insulation. EcoTherm board with a thickness of 100 mm was chosen as the external insulation for the tested walls. A plastic box, fitted with a glow plug at the front side and IRISYS 1002 infrared camera at the back side, was used at the internal side of the tested wall. The glow plug acts as a point heat source and the infrared camera was set to capture 16x16 pixel infrared images at five seconds interval for about an hour. The glow plug's tip temperature as well as the ambient temperature were recorded with a k-type thermocouple and NI USB-TC01 data acquisition system at one second interval.

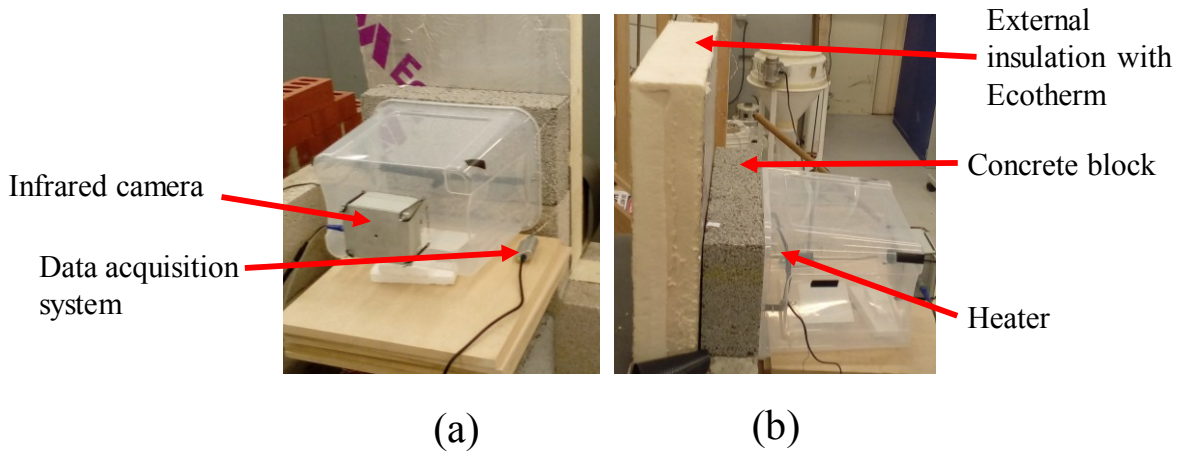

Figure 2: (a) and (b) experimental work on a sample wall.

Figure 2(a) and Figure 2(b) show the experimental work on one of the samples. The sample walls are represented as B1, B2, B3 and B4 for the first run of experiment and C1, C2, C3 and C4 for the second run of experiment. The schematic view of the sample walls are shown in Figures 3(a) to Figure 3(d) and their properties are presented in Table 1. The U-value of the sample walls are calculated using equation (1) where the values of R_i and R_e is considered as 0.13 and 0.04 respectively (Anderson, 2006). The thermal conductivity of the brick wall is taken as 0.27 W/mK (Antoniadis *et al.*, 2012), the thermal conductivity of the concrete block is considered as 1.5 W/mK (ISO 10456, 2007) and the thermal conductivity of the Ecotherm is assumed as 0.022 W/mK (EcoTherm insulation, no date).

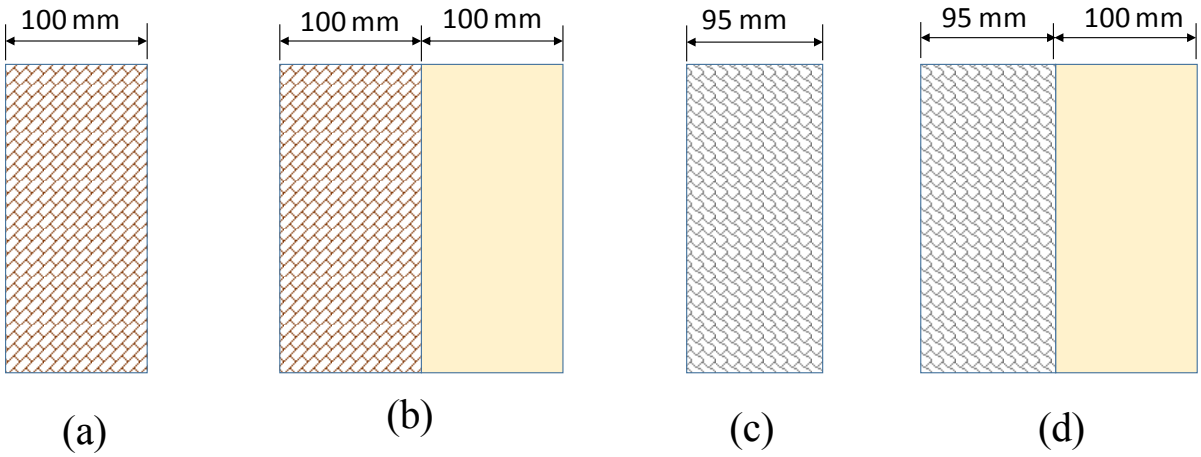

Figure 3: (a) schematic view of samples B1and C1, (b) B2 and C2, (c) B3 and C3 and (d) B4 and C4.

Table 1: Properties of wall sample used in the experiments.

Sample No	Material	Thickness (mm)	Thermal Conductivity (W/mK)	U-value (W/m^2K)
B1 & C1	Brick	100	0.27	1.86
B2 & C2	Brick insulated externally with Ecotherm	100+100 =200	0.27 & 0.22	1.01
B3 & C3	Concrete block	95	1.5	4.29
B4 & C4	Concrete block insulated externally with Ecotherm	95+100 = 195	1.5 & 0.22	1.45

4. Results and Discussion

Samples B4 and C4 have lower U-values than sample B3; therefore, it is expected that the temperature profile of B4 and C4 will be higher than that of B3. The temperature profile of C4 is found clearly higher than that of B3 in Figure 4(a). However, the temperature profile of B4 is marginally higher than that of B3 in figure 4(b), because the ambient temperature was higher during the time of conducting experiment on B3 than on B4.

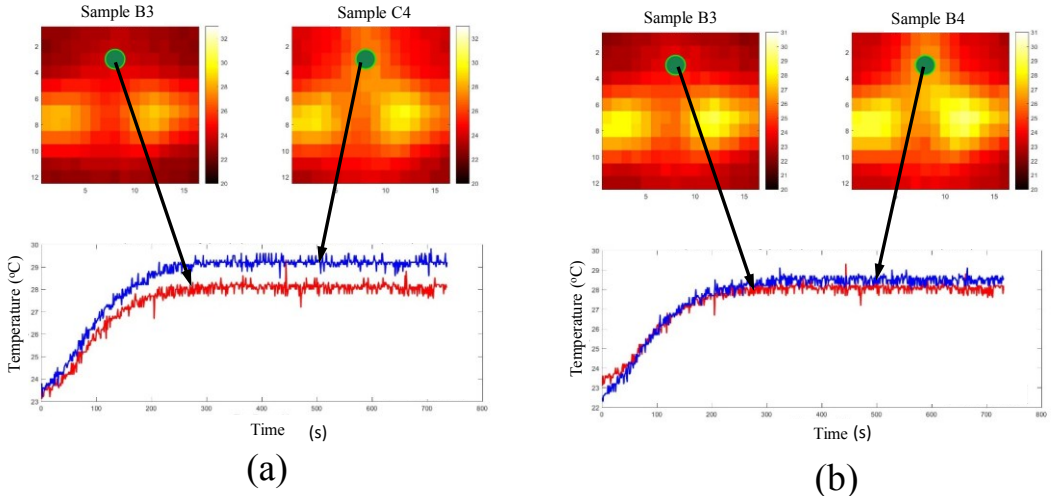

Figure 4: Temperature profiles of (a) sample B3 and C4, (b) B3 and B4

It is also found that the rate of temperature increase with time is higher in samples B4 and C4. Therefore, it is assumed that ambient temperature has a significant influence on the thermal profile and derivative of thermal profile is a key parameter to identify the characteristics of the thermal profile. Considering these assumptions, three modified profiles namely T^a, T^b and T^{ab} are developed, which are presented in equations (2), (3) and (4)

$$\boldsymbol{T}^{a}_{(i,j,k)} = \boldsymbol{T}_{(i,j,k)} - \boldsymbol{T}^{ext}_{k} \qquad (2)$$

$$\boldsymbol{T}^{b}_{(i,j,k)} = \sum_{1}^{k}\left[\boldsymbol{T}_{(i,j,k+1)} - \boldsymbol{T}_{(i,j,k)}\right] \qquad (3)$$

$$T^{ab}_{(i,j,k)} = \sum_1^k [T^a_{(i,j,k+1)} - T^a_{(i,j,k)}] \quad (4)$$

Here $T_{(i,j,k)}$ is the original temperature value at pixel *(i,j,k)* of the infrared image, $T^a_{(i,j,k)}$ is the modified temperature value of pixel *(i,j,k)* of the infrared image, $T^b_{(i,j,k)}$ is the cumulative temperature difference at pixel *(i,j,k)*, $T^{ab}_{(i,j,k)}$ is the cumulative temperature difference of profile T^a and T^{ext}_k is the external temperature at the time of capture of the corresponding infrared image.

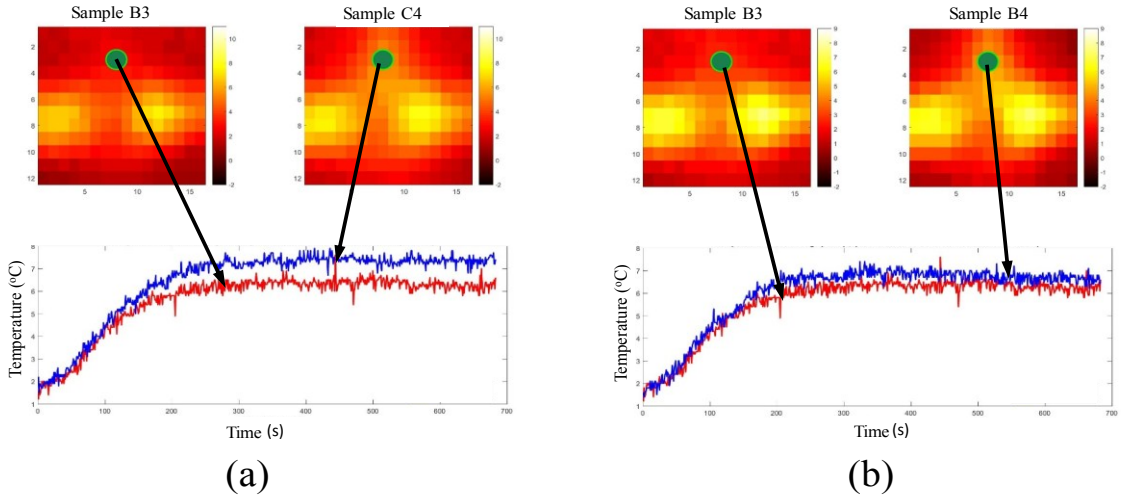

Figure 5: Profiles of T^a(a) sample B3 and C4, (b) B3 and B4

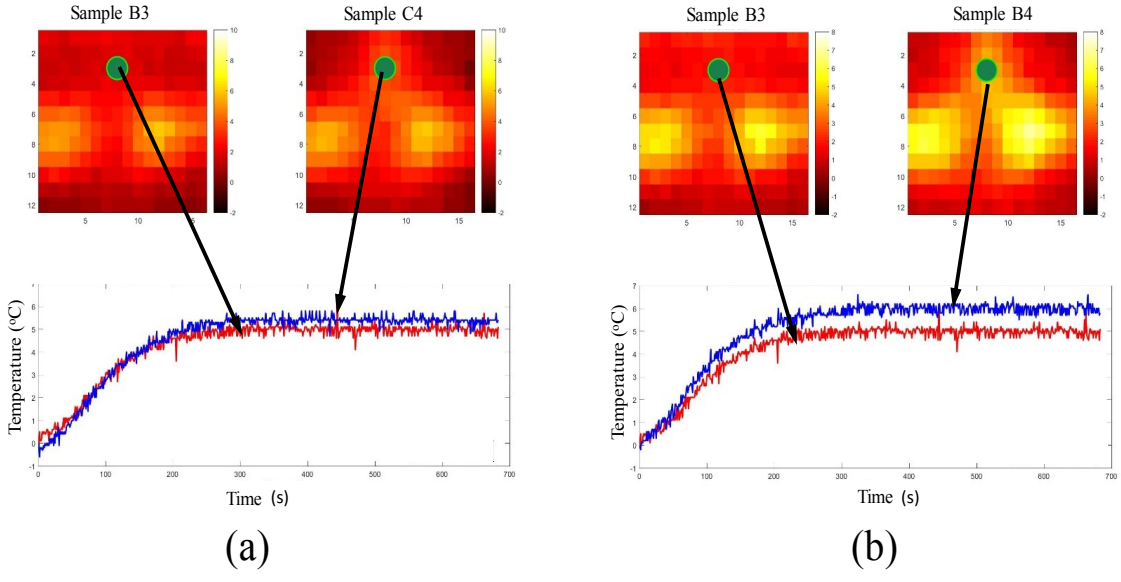

Figure 6: Profiles of T^b(a) sample B3 and C4, (b) B3 and B4

Figure 5(a) shows the profiles T^a of sample B3 and C4 which shows the expected behaviour of the insulated wall's profile which is clearly higher than that of the uninsulated wall. Figure

5(b) shows the same profiles of samples B3 and B4, and it presents a better discrepancy between insulated and uninsulated profiles than that of profile T in Figure 4(b). Figure 6(a) shows the profiles T^b of sample B3 and C4 which shows the expected behaviour of having insulated wall's profile higher than that of uninsulated wall; however, it is not as clearly disguisable as in Figure 4(a) and 5(a).

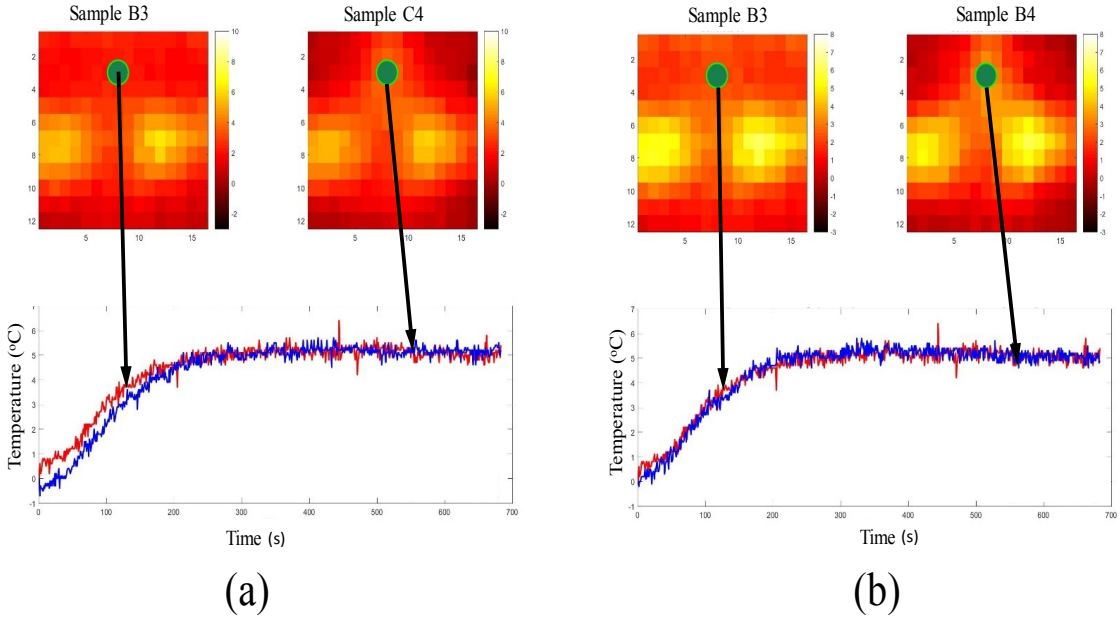

Figure 7: Profiles of T^{ab} (a) sample B3 and C4, (b) B3 and B4

Figure 6(b) shows the same profiles of sample B3 and B4, and it shows clearer discrepancy between insulated and uninsulated profiles than that of profile T and T^a in Figure 4(b) and 5(b) respectively. Figure 7(a) shows the profile T^{ab} of samples B3 and C4, which do not represent any clear distinction. Figure 7(b) also does not represent clear distinction between T^{ab} profiles of sample B3 and B4. A visual comparison of different profiles of the uninsulated wall sample (B3) with two other insulated wall samples (C4 and B4) do not provide an unique solution regarding which profile will show most distinguishable characteristics between insulated and uninsulated walls. Therefore, these visual comparisons of different profiles are extended to 56 randomly chosen points from the infrared images of above eight wall samples. Furthermore, if the temperature profile of the insulated wall is expected to show higher variability than that of the uninsulated wall, the standard deviation of the temperature profile of the insulated wall must be higher than that of the uninsulated wall. Therefore, the standard deviation of wall profiles may convey significant information about the characteristics of the wall type. Hence, the standard deviations of all those profiles of the previously mentioned 56

points are considered for analysis. The results of the analysis of the standard deviations are listed in Table 2 which includes the percentage of cases where the temperature profile of an insulated wall is higher than that of an uninsulated wall.

Table 2: Result of visualisation and standard deviation analysis.

	Profile	Standard deviation of profile
T	57%	86%
T^a	65%	75%
T^b	71%	86%
T^{ab}	47%	80%

It has been found form Table 2 that the standard deviations of profile T and T^b have the highest cases where the profile of an insulated wall is higher than that of an uninsulated wall of about 86%. The reason for this is probably can be explained that both profiles T and T^b have similar dispersion, as the standard deviation represents the dispersion of data.

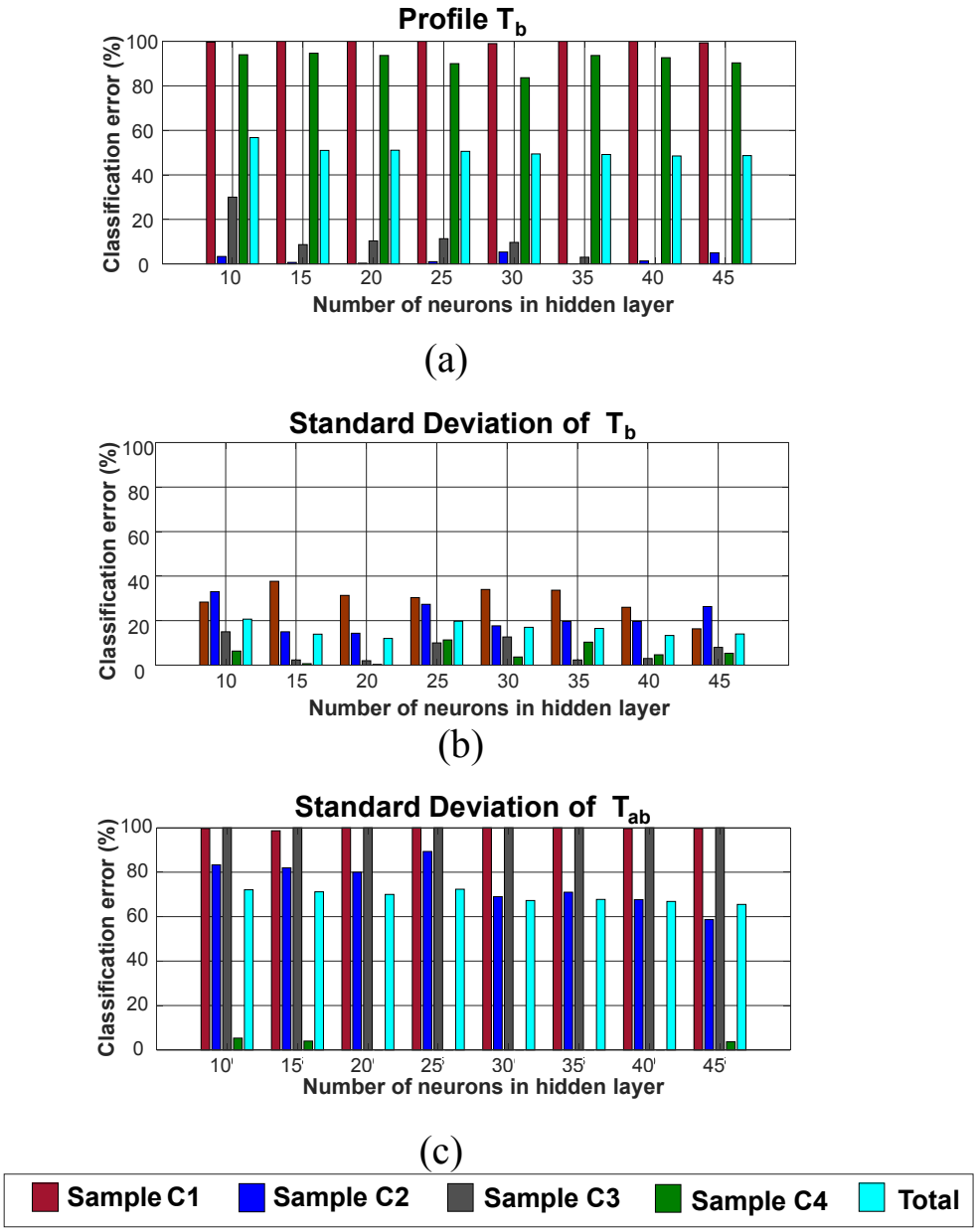

Figure 8: Percentage error of categorisation

The standard deviation of profile T^{ab} has the second highest cases of having higher profile for insulated wall followed by profile T^{b}. Based on this, the standard deviation of T^{b} and standard deviation of T^{ab} are selected for ANN analysis. A feed-forward neural network with softmax layer was programmed using of MATLAB to categorise the wall types with profile T^{b}, the standard deviation of profile T^{b} and the standard deviation of profile T^{ab} as the input parameters and wall types as the output parameters.

Figure 8 (a), (b) and (c) represent the percentage error in categorising the samples C1 C2, C3 and C4 with 10 ,15, 20, 25, 30, 35, 40 and 45 neurons in the hidden layer. It has been found that the standard deviation of profile T^{b} shows the least percentage error when compared to

other profiles. The probable reason for this is that the standard deviation represents the dispersion in the thermal profile more significantly than the profile itself. Profile T^a was developed by deducting the ambient temperature from the original temperature profile, which has reduced the variation that characterises the temperature profile; and hence the percentage error in the categorisation. It has been also found from Figure 8(b) that ANN with 20 neurons in the hidden layer gives the lowest total error of 12% and the error in detecting C1, C2, C3 and C4 are found to be 31%, 14%, 2% and 0.33% respectively.

5. Conclusion

Retrofitting of residential buildings with improved wall insulation could significantly reduce the energy consumption for space heating. However, in-situ measurement of U-value of walls should be considered before retrofitting as over insulation leads to longer payback perioids with more cost and less energy savings. Also this may lead to overheating of building which may forfeit the benefits of retrofitting. The existing methods of U-value estimation have some limitations. Therefore, a novel approach is proposed to categorise the insulation of the walls of buildings based on the U-value by combining thermal image and ANN with the application of point heat source. The inclusion of point heat source in the design ensures the presence of adequate thermal gradient and makes it robust enough to use in all seasons. The results of the presented experiments prove the suitability of feed forward neural network in categorisation of wall insulation and analysing the thermal profiles developed from the thermal images. An ANN with 20 neurons in the hidden layer achieved 88% overall classification accuracy with a minimum accuracy of 69% for any particular wall type.

Reference

Al-Habaibeh, A., Medjdoub, B. and Pidduck, A. (2012) 'Investigating The Influence of Door Design on The Energy Consumption of Buildings Using Infrared Thermography', in *4th. JIIRCRAC 2012, Amman-Jordan, Sept. 10th – 12th 2012*.

Al-Habaibeh, A. and Siena, F. L. (2012) 'The Application of Infrared Thermography for The Evaluation of Insulation and Energy Performance of Buildings', in *4th. JIIRCRAC 2012, Amman-Jordan,*.

Albatici, R. and Tonelli, A. M. (2010) 'Infrared thermovision technique for the assessment of

thermal transmittance value of opaque building elements on site', *Energy and Buildings*, 42(11), pp. 2177–2183. doi: 10.1016/j.enbuild.2010.07.010.

Albatici, R., Tonelli, A. M. and Chiogna, M. (2015) 'A comprehensive experimental approach for the validation of quantitative infrared thermography in the evaluation of building thermal transmittance', *Applied Energy*, 141, pp. 218–228. doi: 10.1016/j.apenergy.2014.12.035.

Anderson, B. (2006) *Conventions for U-value calculations 2006 edition*. 2nd Editio. Scotland UK: BRE Press. Available at: www.bre.co.uk (Accessed: 3 January 2018).

Antoniadis, K. D. *et al.* (2012) 'Improving the Design of Greek Hollow Clay Bricks', *International Journal of Thermophysics*, 33(12), pp. 2274–2290. doi: 10.1007/s10765-012-1294-x.

Asdrubali, F., Baldinelli, G. and Bianchi, F. (2012) 'A quantitative methodology to evaluate thermal bridges in buildings', *Applied Energy*. Elsevier, 97, pp. 365–373. doi: 10.1016/J.APENERGY.2011.12.054.

Baker, P. (2008) *In situ U-value measurements in traditional buildings –preliminary results*. Available at: https://www.historicenvironment.scot/archives-and-research/publications/publication/?publicationId=7fc3d5f6-5992-4106-92bf-a59400bf430c.

BEIS (2018) *Energy Consumption in the UK (ECUK) 2018*, *Energy Consumption in the UK*. Available at: https://assets.publishing.service.gov.uk/government/uploads/system/uploads/attachment_data/file/729317/Energy_Consumption_in_the_UK__ECUK__2018.pdf (Accessed: 14 March 2019).

Biddulph, P. *et al.* (2014) 'Inferring the thermal resistance and effective thermal mass of a wall using frequent temperature and heat flux measurements', *Energy and Buildings*, 78, pp. 10–16. doi: 10.1016/j.enbuild.2014.04.004.

BP (2018) *BP Statistical Review of World Energy*. Available at: https://www.bp.com/content/dam/bp/business-sites/en/global/corporate/pdfs/energy-economics/statistical-review/bp-stats-review-2018-full-report.pdf (Accessed: 21 May 2019).

Campbell Scientific (2012) *Model HFP01 Soil Heat Flux Plate, Instruction Manual*. Available at: http://www.hukseflux.com/sites/default/files/product_manual/HFP01_HFP03_manual_v1620.

pdf.

Chudzik, S. (2012) ‘Measurement of thermal diffusivity of insulating material using an artificial neural network’, *Measurement Science and Technology*, 23(6), pp. 1–11. doi: 10.1088/0957-0233/23/6/065602.

Committee on Climate Change (2016) *UK Climate Action Following the Paris Agreement*. London. Available at: https://www.theccc.org.uk/wp-content/uploads/2016/10/UK-climate-action-following-the-Paris-Agreement-Committee-on-Climate-Change-October-2016.pdf (Accessed: 19 July 2017).

Danielski, I. and Fröling, M. (2015) ‘Diagnosis of Buildings’ Thermal Performance - A Quantitative Method Using Thermography Under Non-steady State Heat Flow’, *Energy Procedia*, 83(83), pp. 320–329. doi: 10.1016/j.egypro.2015.12.186.

Department for Business Energy & Industrial Strategy (2019) *UK becomes first major economy to pass net zero emissions law - GOV.UK*. Available at: https://www.gov.uk/government/news/uk-becomes-first-major-economy-to-pass-net-zero-emissions-law (Accessed: 17 September 2019).

Desogus, G., Mura, S. and Ricciu, R. (2011) ‘Comparing different approaches to in situ measurement of building components thermal resistance’, *Energy and Buildings*, 43(10), pp. 2613–2620. doi: 10.1016/j.enbuild.2011.05.025.

Doran, S. (2001) *DETR Framework Project Report : Prepared for : Safety and Health Business Plan Field investigations of the thermal performance of construction elements as built Approved on behalf of BRE*. Available at: http://projects.bre.co.uk/uvalues/U-values.pdf (Accessed: 17 February 2017).

EcoTherm insulation (no date) *Rigid PIR Thermal Insulation Boards*. Available at: http://www.ecotherm.co.uk/rigid_insulation.aspx (Accessed: 29 April 2018).

Evangelisti, L. *et al.* (2015) ‘In Situ Thermal Transmittance Measurements for Investigating Differences between Wall Models and Actual Building Performance’, *Sustainability*, 7(8), pp. 10388–10398. doi: 10.3390/su70810388.

Ficco, G. *et al.* (2015) ‘U-value in situ measurement for energy diagnosis of existing buildings’, *Energy and Buildings*, 104, pp. 108–121. doi: 10.1016/j.enbuild.2015.06.071.

Fokaides, P. A. and Kalogirou, S. A. (2011) ‘Application of infrared thermography for the

determination of the overall heat transfer coefficient (U-Value) in building envelopes', *Applied Energy*, 88(12), pp. 4358–4365. doi: 10.1016/j.apenergy.2011.05.014.

Fox, M. *et al.* (2014) 'Thermography methodologies for detecting energy related building defects', *Renewable and Sustainable Energy Reviews*, 40, pp. 296–310. doi: 10.1016/j.rser.2014.07.188.

Gaspar, K., Casals, M. and Gangolells, M. (2016) 'A comparison of standardized calculation methods for in situ measurements of façades U-value', *Energy and Buildings*, 130, pp. 592–599. doi: 10.1016/j.enbuild.2016.08.072.

Gori, V. *et al.* (2017) 'Inferring the thermal resistance and effective thermal mass distribution of a wall from in situ measurements to characterise heat transfer at both the interior and exterior surfaces', *Energy and Buildings*, 135, pp. 398–409. doi: 10.1016/j.enbuild.2016.10.043.

Hudson Beale, M., Hagan, M. T. and Demuth, H. B. (2017) *Neural Network Toolbox™ User's Guide*. Online 201. Natick: The MathWorks, Inc. Available at: https://www.mathworks.com/help/pdf_doc/nnet/nnet_ug.pdf.

ISO 10456 (2007) *ISO FDIS 10456:2007(E): Building materials and products — Hygrothermal properties — Tabulated design values and procedures for determining declared and design thermal values*. Available at: http://www.superhomes.org.uk/wp-content/uploads/2016/09/Hygrothermal-properties.pdf (Accessed: 14 May 2018).

Kylili, A. *et al.* (2014) 'Infrared thermography (IRT) applications for building diagnostics: A review', *Applied Energy*, 134, pp. 531–549. doi: 10.1016/j.apenergy.2014.08.005.

Li, F. G. N. *et al.* (2015) 'Solid-wall U -values: heat flux measurements compared with standard assumptions', *Building Research & Information*, 43(2), pp. 238–252. doi: 10.1080/09613218.2014.967977.

Lucchi, E. (2017) 'Thermal transmittance of historical brick masonries: A comparison among standard data, analytical calculation procedures, and in situ heat flow meter measurements', *Energy and Buildings*, 134, pp. 171–184. doi: 10.1016/j.enbuild.2016.10.045.

Nardi, I. *et al.* (2015) 'Validation of quantitative IR thermography for estimating the U-value by a hot box apparatus', *Journal of Physics: Conference Series*, 655, pp. 1–10. doi: 10.1088/1742-6596/655/1/012006.

Nardi, I., Sfarra, S. and Ambrosini, D. (2014) ‘Quantitative thermography for the estimation of the U-value: state of the art and a case study’, *Journal of Physics: Conference Series*, 547, pp. 1–8. doi: 10.1088/1742-6596/547/1/012016.

OECD (2011) *OECD Green Growth Studies Energy*. Available at: https://www.oecd.org/greengrowth/greening-energy/49157219.pdf (Accessed: 21 May 2019).

Sassine, E. (2016) ‘A practical method for in-situ thermal characterization of walls’, *Case Studies in Thermal Engineering*, 8, pp. 84–93. doi: 10.1016/j.csite.2016.03.006.

Tu, J. V. (1996) ‘Advantages and disadvantages of using artificial neural networks versus logistic regression for predicting medical outcomes’, *Journal of Clinical Epidemiology*. Pergamon, 49(11), pp. 1225–1231. doi: 10.1016/S0895-4356(96)00002-9.